[1] J. J. Hopfield and J. M. Worlock, Phys. Rev. 137, A1455 (1965).

[2] D. Frolich and B. Staginnus, Phys. Rev. Letters 19, 496 (1967); D. Frolich, B. Stoginnus, and Y. Onodera, Phys. Status Solidi 40, 547 (1970).

[3] M. Ionue and Y. Toyozawa, J. Phys. Soc. Japan 20, 363 (1965).

[4] T. R. Bader and A. Gold, Phys. Rev. 171, 997 (1968).

[5] R. J. Elliott, Phys. Rev. 108, 1384 (1957); R. J. Elliott and R. London, J. Phys. Chem. Solids 8, 382 (1969).

[6] M. L. Cohen and T. K. Bergstresser, Phys. Rev. 141, 789 (1966); F. H. Pollak, C. W. Higgerbotham, and M. Cardona, J. Phys. Soc. Japan Suppl. 21, 20 (1966).

[7] A. Baldereschi and N. O. Lipari, Phys. Rev. Letters 25, 373 (1970).

[8] A. Baldereschi and N. O. Lipari, Phys. Rev. B 3, 439 (1971).

[9] N. O. Lipari and A. Baldereschi, Phys. Rev. B 3, 2497 (1971).

[10] Throughout the paper we use the notation of G. F. Koster, in *Solid State Physics*, edited by F. Seitz and D. Turnbull (Academic, New York, 1957), Vol. 5.

[11] See, for example, the review by R. S. Knox, in *Solid State Physics*, edited by F. Seitz and D. Turnbull (Academic, New York, 1963), Suppl. 5.

[12] M. Cardona, F. H. Pollak, and K. L. Shaklee, Phys. Rev. Letters 16, 644 (1966); M. Cardona, K. L. Shaklee, and F. H. Pollak, Phys. Rev. 154, 696 (1967).

[13] J. M. Luttinger and W. Kohn, Phys. Rev. 97, 869 (1955).

[14] R. H. Parmenter, Phys. Rev. 100, 573 (1955); G. Dresselhaus, *ibid.* 100, 580 (1955); E. O. Kane, J. Phys. Chem. Solids 1, 249 (1957).

[15] J. M. Luttinger, Phys. Rev. 102, 1030 (1956).

[16] G. Dresselhaus, A. F. Kip, and C. Kittel, Phys. Rev. 98, 368 (1955).

[17] L. D. Landau and E. M. Lifshitz, *Quantum Mechanics* (Pergamon, Oxford, 1965), Chap. 5.

[18] A. P. Yutsis, I. B. Levinson, and V. V. Vanagas, *The Theory of Angular Momentum* (NSF, U.S. GPO, Washington, 1962).

[19] N. O. Lipari and A. Baldereschi, Phys. Rev. Letters 25, 1660 (1970).

[20] P. J. Dean, C. H. Henry, and C. J. Frosh, Phys. Rev. 168, 812 (1968).

[21] W. J. Turner and W. E. Reese, Phys. Rev. 127, 126 (1962).

[22] R. G. Stafford and K. Park, Phys. Rev. Letters 25, 1652 (1970).

PHYSICAL REVIEW B VOLUME 6, NUMBER 10 15 NOVEMBER 1972

X-Ray Photoemission Measurements of GaP, GaAs, InAs, and InSb

T. Lane
Air Force Institute of Technology, Wright-Patterson Air Force Base, Ohio 45433

and

C. J. Vesely and D. W. Langer
Aerospace Research Laboratories, Wright-Patterson Air Force Base, Ohio 45433

(Received 31 May 1972)

X-ray-induced electron-emission measurements were used to determine the energy levels of core electrons in GaP, GaAs, InAs, and InSb. The investigated energy range extends from the bottom of the valence band to about 1400 eV below the Fermi level. Samples were cleaned by using argon-ion bombardment, and the gold $4f_{7/2}$ electron level was used to provide an energy reference level. Chemical shifts were determined by comparing the results with previously published experimental values for the pure elements. Several spin-orbit-splitting values were experimentally determined. Two maxima in the conduction-band density of states were located with respect to the bottom of the conduction band by comparing the photoemission data for the outermost core d and p electrons with transition energies measured by uv absorption, uv reflectivity, and electron-energy-loss experiments. One maximum is located between 0.8 and 1.4 eV above the bottom of the conduction band depending on the compound and the other is located between 3 and 4 eV.

I. INTRODUCTION

We present the results of our x-ray-induced electron-emission studies of the electron-core levels of GaP, GaAs, InAs, and InSb. Similar measurements on several of the II-VI compounds have previously been reported.[1]

Section II includes a brief description of the apparatus and principles of operation along with a more detailed description of sample preparation and energy calibration. Sample preparation included cleaning by ion bombardment and energy calibration was based on the $4f_{7/2}$ energy level of gold.

The results of our measurements are listed in Sec. III which is divided into three sections. Section III A is concerned with the actual location of the measured energy levels. We list our results and compare them with published experimental data for the pure elements. Spin-orbit-splitting values are listed and discussed in Sec. III B. Section III C concerns the outermost core levels of the measured compounds. Structure in the density of conduction states is located with respect to the bottom of the conduction band by comparing our results for these levels with transition energies measured by uv absorption,[2] uv reflectivity,[3] and electron-energy-loss[4] experiments. The principal results of our measurements are summarized in Sec. IV.

II. EXPERIMENTAL PROCEDURE

A. Apparatus

Our measurements were made with a modified version of the Varian Associates induced-electron-emission (IEE) spectrometer discussed in previous papers.[1,5] An aluminum x-ray anode and an analyzer potential of 100 V were used yielding an effective resolution of 1.75-eV full width at half-maximum for the carbon 1*s* peak in graphite.

The modified apparatus was equipped with a turbomolecular pump in addition to a liquid-nitrogen-trapped mechanical forepump and a titanium-sublimation pump. With this arrangement the pressure in the main chamber was maintained in the mid-10^{-7}-Torr range during measurements and it was possible to efficiently pump inert gases during sample preparation. Another modification to the system was the addition of a second vacuum chamber which allowed the preparation and transfer of samples inside the vacuum system. A Varian temperature-control unit was also used to maintain samples at a constant temperature during preparation.

B. Principles of Operation

The principles of operation have been previously discussed.[1,6] X rays from the aluminum anode interact photoelectrically with electrons in the sample. The binding energy E_b of these electrons is determined by applying the relationship

$$E_b = E_{\mathrm{x\ ray}} - E_{\mathrm{kin}} - \phi_{\mathrm{sp}} - \phi , \tag{1}$$

where $E_{\mathrm{x\ ray}}$ is the x-ray energy, E_{kin} is the measured kinetic energy of the electrons emitted from the sample, ϕ_{sp} is the work function of the analyzer, and ϕ is the charge buildup which occurs on a sample which is not a conductor. In this equation, E_b is determined with respect to the Fermi level of the measured sample.

We sputtered a thin layer of gold onto the surface of all the samples and used the Au $4f_{7/2}$ value of 83.9 eV[7] as an energy reference value in order to determine the quantity $\phi_{\mathrm{sp}} + \phi$ for each sample. The details of this procedure are the same as those previously described[1] except that gold is now used as the reference material instead of carbon. From the scatter in our measurements we estimate that this technique allows us to determine the peak locations to within ± 0.2 eV (not including systematic errors). The calculated standard deviation (σ) is shown in the tables for those levels where the scattering in measurements yielded a value greater than ± 0.2 eV.

C. Sample Preparation

Prior to making measurements, the samples were cleaned in an argon atmosphere by ion bombardment. Using a dc diode arrangement, a potential of 4 kV was applied between the sample and a wire loop surrounding the sample. A pressure of 20 mTorr of argon was maintained during a sputtering period of about 10 min and during this time the sample was maintained at a temperature of 10 °C. For this process, the samples were cut into 8-mm-thick platelets and were attached with an adhesive to a four-sided copper sample holder in such a way as to cover the entire surface area of the sample holder which contributes to the measurement.

The sputtering technique was also used to deposit the thin layer of gold on the sample which was used in the energy-calibration procedure. In this case the sample was positioned within a gold-lined cylinder and at 35 mTorr and 2 kV, the process took between 10 and 20 sec. A schematic diagram of the sample preparation chamber is shown in Fig. 1.

The effectiveness of the "cleaning" technique was determined by comparing the count rates for the oxygen 1*s*, carbon 1*s*, and sample levels prior to and after sputtering. Figure 2 shows three overlapped spectra taken on a GaP sample before sputtering. The spectra were all plotted with the

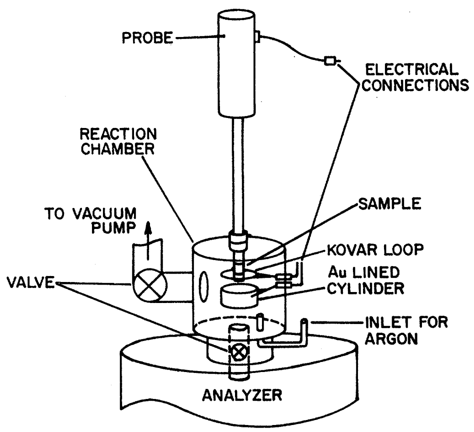

FIG. 1. Schematic diagram of the sample preparation chamber showing the arrangement used for ion bombardment.

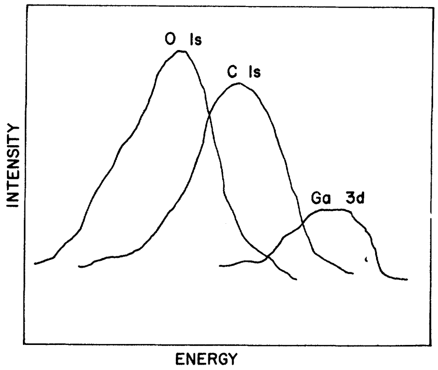

FIG. 2. Relative intensities of the oxygen 1*s*, carbon 1*s*, and gallium 3*d* peaks as observed before sputtering. The peaks have been arbitrarily shifted along the energy axis in order to aid comparison.

same gain and are labeled on the figure. As can be seen, the oxygen and carbon peaks are quite large in comparison with the gallium 3*d* peak. After sputtering we duplicated these measurements and the results are shown in Fig. 3. Again, all three spectra were plotted with the same gain but now the carbon and oxygen peaks are barely detectable. The same type of results were obtained for all four compounds.

In addition to the large decrease in carbon and oxygen, the sputtering increased the sample counting rates so that in several cases, sample levels were measurable which would not have been so without sputtering. For example, Fig. 4 shows a spectrum taken of InSb before sputtering. The antimony 3*d* peaks are very small and lie to either side of the large oxygen 1*s* peak. Figure 5 shows the lower energy half of this energy range measured after sputtering. The large peak is the antimony $3d_{5/2}$ level and the oxygen is now barely detectable at about 532 eV.

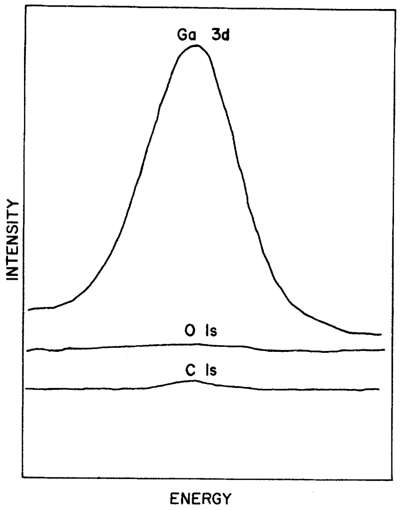

FIG. 3. Relative intensities of the oxygen 1*s*, carbon 1*s*, and gallium 3*d* peaks as observed after sputtering. The peaks have been arbitrarily shifted along the energy axis in order to aid comparison.

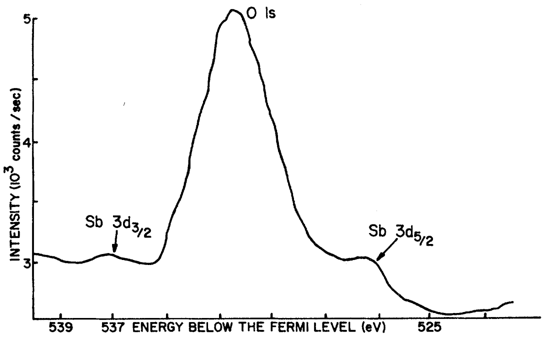

FIG. 4. Observed spectrum for InSb before sputtering (524–539 eV below the Fermi level).

III. DISCUSSION OF RESULTS

A. Electron-Core Levels

The results of our measurements are shown in Tables I–III. These tables list the values that we were able to obtain for gallium, indium, phosphorus, arsenic, and antimony electron-core levels in the compounds along with experimental values for the pure elements as reported by Bearden and Burr.[8] All values are given with respect to the Fermi level of the material measured. The columns headed by E_d list the energy differences between our measured values for the compounds and the published values for the element.

All of the gallium and indium levels were found to have shifted toward higher binding energies compared to the pure elements. Also, with the exception of the arsenic 3*s* level, all the arsenic and phosphorus levels have shifted toward lower binding energies. Our results for antimony give both small

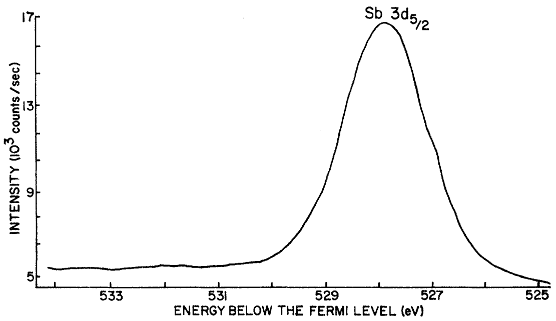

FIG. 5. Observed spectrum for InSb after sputtering (525–534 eV below the Fermi level).

TABLE I. Electron-core levels of gallium in metallic gallium and in the measured gallium compounds. Energy values are in eV and are given with respect to the Fermi level of each material. The differences between the measured values for the compounds and the values for the metal are listed in the columns headed by E_d.

Level	Ga metal[a]	GaAs[b]	E_d[c]	GaP[b]	E_d[c]
$3d_{5/2}$	17.4 ± 0.5	18.8	(1.62)	18.66	(1.52)
$3d_{3/2}$		19.37		19.33	
$3p_{3/2}$	102.9 ± 0.5	104.26	1.36	104.12	1.22
$3p_{1/2}$	106.8 ± 0.7	107.94	1.14	107.66	0.86
$3s$	158.1 ± 0.5	159.58	1.48	159.45	1.35
$2p_{3/2}$	1115.4 ± 0.5	1116.7	1.3	1116.6	1.2
$2p_{1/2}$	1142.3 ± 0.5	1143.59	1.29	1143.44	1.14
$2s$	1297.7 ± 1.1	1301.04	3.34	1301.13	3.43

[a] From a tabulation of experimental data in Ref. 8.

[b] Present work on Ga compounds.

[c] Those values enclosed by parentheses were calculated by taking the difference between the weighted average of the measured values for a compound and the value for the metal.

positive and negative shifts. It appears that the previously reported values for pure antimony and the 3*s* level in pure arsenic may be in error. In general, it is apparent that the magnitude of the energy shifts determined for these compounds is less than that which was observed in our previous work on the II-VI compounds.[1] This is expected since the bonding in these crystals is less ionic.

B. Spin-Orbit Splitting

The spin-orbit-splitting values that we were able to obtain for many of the levels we measured are listed in Tables IV and V. These tables also include experimental values for the pure elements as compiled by Bearden and Burr,[8] some experimental values for the compounds obtained from optical absorption measurements as reported by Cardona *et al.*[2] and theoretical values for the free atoms calculated by Herman and Skillman[9] using a first-order perturbation treatment. Although strict agreement is not to be expected with the theoretical calculations,[10] agreement is nevertheless relatively good except for the 3*p* and 4*p* levels of antimony.

Except for the arsenic 3*p* levels, agreement between our values and those listed in Bearden and Burr's table of electron binding energies is very good. Agreement with Cardona's values is also good. As with the II-VI compounds we were unable to detect any significant variation in the magnitude of the splittings among the compounds or when compared with the pure elements.

C. Density of States

In a series of absorption and reflectivity measurements in the far uv, Cardona and co-workers[2,3] observed structure which they attributed to transitions from the outer core levels of these materials to at least two locations in the conduction band. In particular, they attribute one peak to the flat region in the vicinity of the X_1 point and another

TABLE II. Electron core levels of indium in metallic indium and in the measured indium compounds. Energy values are in eV and are given with respect to the Fermi level of each material. The differences between the measured values for the compounds and the values for the metal are listed in the columns headed by E_d.

Level	In[a] metal	InAs[b]	E_d[c]	InSb[b]	E_d[c]
$4d_{5/2}$	16.2 ± 0.3	17.09	(1.28)	16.96	(1.13)
$4d_{3/2}$		18.07		17.89	
$4p_{3/2}$	...	84.57	...	84.52	...
$4p_{1/2}$	77.4 ± 0.4	78.07	0.67	78.02	0.62
$4s$	121.9 ± 0.3	122.70	0.80	122.58	0.68
$3d_{5/2}$	443.1 ± 0.3	443.97	0.87	443.86	0.76
$3d_{3/2}$	450.8 ± 0.3	451.59	0.79	451.47	0.67
$3p_{3/2}$	664.3 ± 0.3	665.29	0.99	665.25	0.95
$3p_{1/2}$	702.2 ± 0.3	702.89	0.69	703.08	0.88
$3s$	825.6 ± 0.3	826.40	0.80	826.66	1.06

[a] See Ref. a, Table I.

[b] Present work on In compounds.

[c] See Ref. c, Table I.

TABLE III. Electron core levels of P, As, and Sb in the measured compounds and in the pure materials. Energy values are in eV and are given with respect to the Fermi level of each material. The differences between the measured values for the compounds and the values for the pure materials are listed in the columns headed by E_d.

Level	(*X*)[a]	Ga(*X*)[b]	E_d[c]	In(*X*)[b]	E_d[c]
P $2p_{3/2}$	132.2 ± 0.5	128.65	(−3.25)	...	...
P $2p_{1/2}$		129.54		...	...
P $2s$	189.3 ± 0.4	186.45	−2.85	...	...
As $3d_{5/2}$	41.2 ± 0.7	40.78	(−0.11)	40.59	(−0.31)
As $3d_{3/2}$		41.55		41.33	
As $3p_{3/2}$	140.5 ± 0.8	140.0	−0.5	139.85	−0.65
As $3p_{1/2}$	146.4 ± 1.2	145.02	−1.38	144.79	−1.61
As $3s$	203.5 ± 0.7	204.17	+0.67	203.86	+0.36
As $2p_{3/2}$	1323.1 ± 0.7	1322.27	−0.83	1322.12	−0.98
As $2p_{1/2}$	1358.6 ± 0.7	1357.92	−0.68	1357.78	−0.82
Sb $4d_{5/2}$	31.40 ± 0.3	...	...	31.44	(+0.58)
Sb $4d_{3/2}$		...	...	32.8	
Sb $4p_{3/2}$	98.4 ± 0.5	...	...	99.1	0.7
Sb $4p_{1/2}$	...	...	...	109.21	...
Sb $4s$	152.0 ± 0.3	...	...	152.5	0.5
Sb $3d_{5/2}$	527.5 ± 0.3	...	...	527.4	−0.1
Sb $3d_{3/2}$	536.9 ± 0.3	...	...	536.83	−0.07
Sb $3p_{3/2}$	765.6 ± 0.3	...	...	765.74	0.14
Sb $3p_{1/2}$	811.9 ± 0.3	...	...	811.98	0.08
Sb $3s$	943.7 ± 0.3	...	...	943.7 ± 0.4	0.0

[a] Same as Ref. a in Table I. (*X*) represents P, As, or Sb.

[b] Present work on the III-V compounds.

[c] Same as Ref. c in Table I.

TABLE IV. Measured spin-orbit-splitting values for Ga and In. Also included are other experimental values which are available (including values for the pure elements) and theoretical values obtained by Herman and Skillman. All values are in eV.

Level	P[a]	As[a]	Sb[a]	Element[b]	Free atom[c] (theory)
Ga 3*d*	0.67(0.6)[d]	0.57	...	...	0.53
Ga 3*p*	3.54(3.3)[d]	3.68(3.6)[d]	...	3.9	3.69
Ga 2*p*	26.84	26.89	...	26.9	27.83
In 4*d*	...	0.98(1.0)[d]	0.93(0.9)[d]	...	0.97
In 4*p*	...	6.5	6.5	...	6.39
In 3*d*	...	7.62	7.61	7.7	8.19
In 3*p*	...	37.6	37.83	37.9	36.05

[a] Present work on the III-V compounds (except values in parentheses).

[b] From a tabulation of experimental data in Ref. 8.

[c] From Ref. 9.

[d] Experimental data on the III-V compounds from Ref. 2.

peak to a similar region near the L_3 point. By using our electron-emission data which give the energy values for the initial states, it should be possible to use the transition energies to locate with respect to a known point in the band structure, namely, the bottom of the conduction band, the locations of the maxima in the conduction-band density of states. We also apply our results to the electron-energy-loss measurements of Festenberg[4] in the same manner.

The results of such an analysis are shown in Table VI. The column headed by "core level IEE" lists the results of our measurements for the outer core levels. All the values in the table are given in eV and the photoemission values are given with respect to the Fermi level. There are two columns headed by "Transition energy I" and "Transition energy II." These columns list the two sets of transition energies from the core levels as measured by uv absorption, uv reflectivity, and electron-energy-loss experiments. Since we have shown in our previous x-ray and uv photoemission work on the II-VI compounds[11] that the effective location of the Fermi level is at the center of the band gap during our measurements, by adding one-half the band-gap energy to our values and subtracting the result from the indicated transition energies, we obtain the location of the final states of these transitions with respect to the bottom of the conduction band. As Table VI shows, two peaks are observed in the density of states. One peak is located between 0.8 and 1.4 eV above the bottom of the conduction band depending on the material. The other, shown in the last column, is located another 1.5–2.5 eV higher yet or about 3–4 eV above the bottom of the condution band. An important point here is that the higher peak in the density of states was only observed in transitions from the outermost *d* levels of the cation. That is, by using our measured values for the initial states of the transitions from the Ga 3*p*, P 2*p*, As 3*d*, and Sb 4*d* levels, we were able to establish that all of the observed transitions from these levels only go to the lower peak in the conduction-band density of states. Since the resolution in the uv and electron-energy-loss experiments was claimed to be sufficient to have detected transitions to the second peak, one is left with the problem of explaining why these transitions were not observed. Should the matrix elements involved have such different values?

We have taken the final-state energy values for both peaks in the density of states and plotted them on band-structure diagrams published by Cohen and Bergstresser,[12] who have made pseudopotential calculations for these crystals. Since the results are very similar for the two gallium compounds and for the two indium compounds, we only show one diagram for each. Figure 6 shows InSb. The grey bands indicate the positions of the peaks and their width represents the spread in the reported transition energy values. As can be seen, the lower peak in the density of states appears to lie

TABLE V. Measured spin-orbit-splitting values for P, As and Sb. Also included are other experimental values which are available (including values for the pure elements) and theoretical values obtained by Herman and Skillman. All values are in eV.

Level	Ga[a]	In[a]	Element[b]	Free atom[c] (theory)
P 2*p*	0.89	...	...	0.95
As 3*d*	0.77	0.74	...	0.81
As 3*p*	5.02	4.94	5.9	5.09
As 2*p*	35.65	35.66	35.5	36.52
Sb 4*d*	...	1.36(1.4)[d]	...	1.38
Sb 4*p*	...	10.11	...	8.19
Sb 3*d*	...	9.43	9.4	10.09
Sb 3*p*	...	46.24	46.3	43.58

[a] See Ref. a in Table IV.

[b] See Ref. b in Table IV.

[c] See Ref. c in Table IV.

[d] See Ref. d in Table IV.

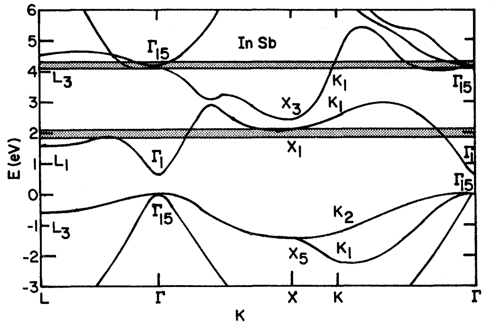

FIG. 6. Calculated band structure for InSb (from Ref. 12). The shaded areas show the experimentally determined regions with a high density of states.

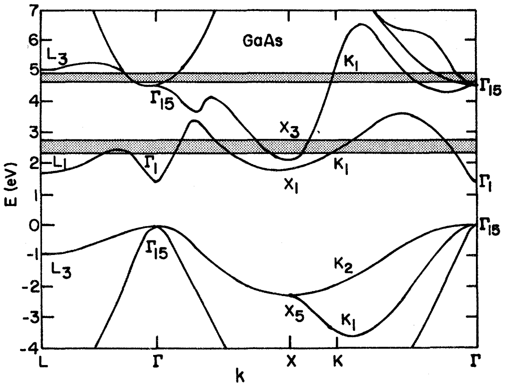

FIG. 7. Calculated band structure for GaAs (from Ref. 12). The shaded areas show the experimentally determined regions with a high density of states.

in a region extending from just above the L_1 point up to the area of the $X_1 - X_3$ points and the upper peak is located just below the L_3 region. The same holds true for InAs except that the spread in the transition-energy values is larger. Figure 7 shows the results for GaAs. Except for one difference, both peaks in the density of states appear to be situated in the same position relative to the band structure as for the indium compounds. The difference is that the calculated X_1 and X_3 points

TABLE VI. Regions in the conduction band (cb) with a high density of vacant states determined by comparing the results of x-ray-induced electron emission with transition energies measured by optical absorption and reflectivity and electron-energy-loss measurements. All values are in eV and the photoemission values are given with respect to the Fermi level.

Compound	Level	Core level IEE	Transition energy I	Peak I above cb min.	Transition energy II	Peak II above cb min.
GaP	Ga $3d_{5/2}$	18.7	20.6^a	0.8		
	$3d_{3/2}$	19.3	21.2^a	0.8		
	$3d$	(18.9)	20.9^b	0.9	23.2^b	3.2
			21.3^c	1.3	23.3^c	3.3
					23.1^a	3.1
	$3p_{3/2}$	104.1	106.1^a	0.9		
	$3p_{1/2}$	107.7	109.4^a	0.6		
	P $2p$	(128.9)	131.2^a	1.2		
GaAs	Ga $3d$	(19.0)	20.9^a	1.2	23.0^a	3.3
			20.6^b	0.9	22.9^b	3.2
			21.0^c	1.3	23.2^c	3.5
	$3p_{3/2}$	104.3	106.2^a	1.2		
	$3p_{1/2}$	107.9	109.8^a	1.2		
	As $3d$	(41.1)	43.1^a	1.3		
InAs	In $4d_{5/2}$	17.1	18.5^a	1.2	21.55^a	4.25
			18.5^b	1.2	21.3^b	4.0
	$4d_{3/2}$	18.1	19.5^a	1.2	22.3^a	4.0
			19.4^b	1.1	22.1^b	3.8
	$4d$	(17.5)	19.6^c	1.9	21.6^c	3.9
	As $3d$	(40.9)	43^a	1.9		
InSb	In $4d_{5/2}$	17.0	18.3^a	1.2	20.8^a	3.7
	$4d_{3/2}$	17.9	19.2^a	1.2	21.5^a	3.5
	$4d$	(17.3)	18.9^b	1.5	20.9^b	3.5
			19.1^c	1.3	21.0^c	3.6
	Sb $4d_{5/2}$	31.4	32.9^a	1.4		
	$4d_{3/2}$	32.8	34.3^a	1.4		

[a] Optical absorption, from Ref. 2. [b] Optical reflectivity, from Ref. 3. [c] Electron energy loss, from Ref. 4.

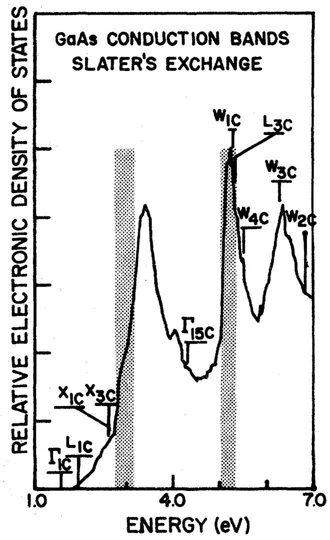

FIG. 8. Calculated density of conduction states for GaAs using Slater's exchange (from Ref. 13). The shaded areas show the experimentally determined regions with a high density of states.

are a little lower with respect to the lower peak in the density of states instead of a little higher as in the indium compounds. The same thing is true for GaP.

Although the shape of the spectra obtained by absorption and reflectivity measurements is determined in part by transition matrix elements, it should be meaningful to directly compare peaks in calculated density-of-states distributions for these materials with the values presented in Table VI. Such comparison is shown in Fig. 8. The theoretical curve was calculated by Stukel, Collins, and Euwema[13] based on a self-consistent orthogonalized plane-wave procedure with Slater's exchange approximation. It does not include transition matrix elements. They found three main peaks in the first 6 or 7 eV of the conduction band. The lowest peak comes from the *K*-point region, the middle peak from the *L*-point region, and the third peak from the *K* region. The experimental data are again superimposed in grey. Only the locations of the peaks are being compared and not their magnitudes. The lower peak falls higher than the calculated $X_1 - X_3$ points but below, by a few tenths of an eV, the lowest calculated peak. The next-to-lowest calculated peak almost exactly coincides with the second peak observed in the data. The same authors also made calculations using Kohn–Sham's exchange constant and the results are shown in Fig. 9. Although the lowest calculated peak is in closer agreement with the data than when using Slater's exchange, the upper peaks are in worse agreement.

Density-of-states curves have also been calculated by Higginbotham, Pollak, and Cardona for InSb and InAs[14] using a modified $\vec{k}\cdot\vec{p}$ method. Agreement is excellent (within 0.2 eV) for InSb but the experimental peaks are both about 0.8 eV lower than the corresponding theoretical peaks for InAs.

IV. CONCLUSIONS

The results of our x-ray-induced electron-emission studies of GaP, GaAs, InAs, and InSb are summarized in this section. First, we found that the amount of oxygen and carbon on the surface of the samples could be significantly reduced along with a large increase in sample counting rates by using the process of ion bombardment to clean the samples. A thin layer of gold sputtered on the surface of the samples allowed us to use the gold $4f_{7/2}$ level as a reference level.

All the measured core levels of gallium and indium were found to have shifted toward higher binding energies compared to the pure elements. Except for the arsenic 3*s* level, the measured arsenic and phosphorus levels shifted toward lower binding energies. Small shifts in both directions were observed for antimony. All of these shifts with the exception of the As 3*s* level and the antimony levels can be understood by considering the partial ionic character of the bonding in these crystals.

Several spin-orbit-splitting values were measured including some for the first time. No significant variation in the magnitude of the splittings was observed among the compounds or when com-

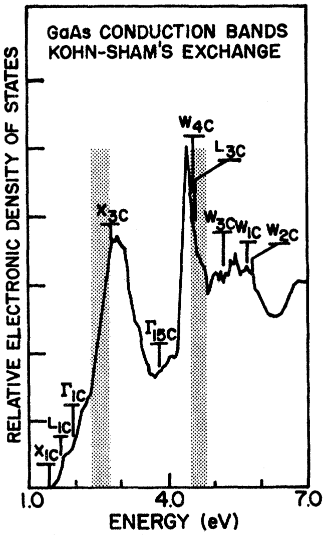

FIG. 9. Calculated density of conduction states for GaAs using Kohn–Sham's exchange (from Ref. 13). The shaded areas show the experimentally determined regions with a high density of states.

pared with the pure elements.

Two maxima in the conduction band density of states were located with respect to the bottom of the conduction band by comparing our data for the outermost core *d* and *p* electrons for these compounds with transition energies measured by uv absorption, uv reflectivity, and electron-energy-loss experiments. One maximum is located between 0.8 and 1.4 eV above the bottom of the conduction band depending on the material and the other is located between 3 and 4 eV. This analysis showed that the higher peak was only observed in transitions from the outermost *d* levels of the cation while the lower peak was observed in transitions from all of the core levels for which data were available. Both peaks correspond rather closely with the two lowest maxima which have been obtained in published density-of-states calculations for some of these compounds.

ACKNOWLEDGMENTS

We wish to thank T. C. Collins for helpful discussions. We also wish to thank B. Terrants of the U.S. Air Force Materials Laboratory for furnishing the GaP and M. Davis of the U.S. Air Force Avionics Laboratory for furnishing the GaAs.

---

[1] C. Vesely and D. Langer, Phys. Rev. B 4, 451 (1971).

[2] M. Cardona, W. Gudat, B. Sonntag, and P. Yu, in *Proceedings of the Tenth International Conference on the Physics of Semiconductors, Cambridge, Massachusetts*, 1970, edited by S. Keller, J. Hensel, and F. Stern (U.S. AEC, Oak Ridge, Tenn., 1970), p. 209.

[3] M. Cardona, W. Gudat, E. E. Koch, M. Skibowski, B. Sonntag, and P. Y. Yu, Phys. Rev. Letters 25, 659 (1970).

[4] C. V. Festenberg, Z. Physik 227, 453 (1969).

[5] J. Helmer and N. Weichert, Appl. Phys. Letters 13, 266 (1968).

[6] D. Langer and C. Vesely, Phys. Rev. B 2, 4885 (1970).

[7] M. O. Krause (private communication).

[8] J. Bearden and A. Burr, Rev. Mod. Phys. 39, 125 (1967).

[9] F. Herman and S. Skillman, *Atomic Structure Calculations* (Prentice-Hall, Englewood Cliffs, N. J., 1963).

[10] F. Herman, C. Kuglin, K. Cuff, and R. Kortum, Phys. Rev. Letters 11, 541 (1963).

[11] C. Vesely, R. Hengehold, and D. Langer, Phys. Rev. B 5, 2296 (1972).

[12] M. Cohen and T. Bergstresser, Phys. Rev. 141, 789 (1966).

[13] D. Stukel, T. Collins, and R. Euwema, in *Electronic Density of States*, edited by L. Bennett, Natl. Bur. Std. (U. S.) Spec. Publ. 323 (U. S. GPO, Washington, D. C., 1971), p. 93.

[14] C. Higginbotham, F. Pollak, and M. Cardona, in *Proceedings of the Ninth International Conference on the Physics of Semiconductors, Moscow*, 1968 (Viniti, Moscow, 1968), p. 57.

PHYSICAL REVIEW B VOLUME 6, NUMBER 10 15 NOVEMBER 1972

Study of the Homology between Silicon and Germanium by Thermal-Neutron Spectrometry

G. Nilsson and G. Nelin
Aktiebolaget Atomenergi, Studsvik, Sweden

(Received 5 May 1972)

The phonon dispersion relations in silicon and germanium are found to be nearly homologous with small but significant deviations. These results, which have been obtained by thermal-neutron spectrometry, are strongly supported by an analysis in which comparison is made with elastic constants, heat capacities, and Raman frequencies for these elements. Previously observed discrepancies between results obtained from shell-model calculations and from heat-capacity measurements are explained. Attempts are made to elucidate the origin of the observed differences between the dimensionless phonon frequencies of group-IV*B* elements with the diamond-type crystal structure.

I. INTRODUCTION

A perturbation expansion, based on tight-binding electron wave functions in the Hartree–Fock approximation, was used by Tolpygo[1] to establish a lattice-dynamical theory for homopolar crystals of the diamond type. The equations of motion were shown by Cochran[2] to be equivalent to the corresponding equations of the shell model; each atom is here represented by a point-ion core surrounded by a rigid spherical shell of valence electrons. In the harmonic approximation short-range forces are established by introducing spring constants allowing for core-core, core-shell, and shell-shell interactions; long-range forces are described by bare electrostatic core-core, core-